SSRG International Journal of Civil Engineering
ISSN: 2348-8352/ https://doi.org/10.14445/23488352/IJCE-V12I5P109

Volume 12 Issue 5, 99-113, May 2025

Original Article

Adsorption of PFOA and PFOS on Chitosan-Carbon Nanotubes Hydrogel Beads: Parametric Optimization Using RSM

Siphesihle Mangena Khumalo[1], Babatunde Femi Bakare[1,2], Sudesh Rathilal[1]

[1]*Green Engineering Research Group, Durban University of Technology, Durban, South Africa.*
[2]*Environmental Pollution and Remediation Research Group, Mangosuthu University of Technology, Durban, South Africa.*

[1]*Corresponding Author : SiphesihleK1@dut.ac.za*

Received: 07 March 2025 Revised: 09 April 2025 Accepted: 08 May 2025 Published: 31 May 2025

Abstract *- The environmental occurrence of perfluorooctanoic acid (PFOA) and perfluorooctane sulfonic acid (PFOS), particularly in potable water sources, is evidence that current wastewater treatment facilities are unable to eliminate these newly recognized environmental contaminants entirely. On the other hand, studies on parametric optimization for solid-liquid adsorption of PFOA and PFOS are scanty. As such, the present study focuses on the parametric optimization of PFOA and PFOS on chitosan-carbon nanotube hydrogel beads from aqueous solution using the central composite design in response surface methodology as the first case. The effect of solution pH (4 – 10), contact time (2 – 48 hours), adsorbate initial concentration (5-20 mg/L), and adsorbent load (0.05 – 1.5 g/L) on the uptake of PFOA and PFOS were investigated using batch adsorption studies. The experimental data were analysed using variance alongside quadratic response models, resulting in R^2 values higher than 0.97 with 95% confidence. The study gave optimal conditions of pH 4, contact time of 48 hours, adsorbate concentration of 5 mg/L, adsorbent load of 1.5 g/L, and percentage removals of greater than 90% at a standard deviation of ±1% for both PFOA and PFOS. As such, the present study's findings under optimal conditions indicate that proper adjustment of operating parameters is crucial in maximizing the uptake of the model adsorbate.*

Keywords *- Perfluorooctanoic acid, Perfluotorooctane sulfonic acid, Chitosan, Carbon nanotube, Response surface methodology.*

1. Introduction

Per- or poly-Fluoroalkyl Substances (PFAS) are a group of man-made, persistent organo-fluorine compounds. These compounds consist of an alkyl chain that is either fully or partially fluorinated and terminates in a polar acid functional group, such as carboxylate, sulfonate, or phosphonate, as documented by Garg et al. [1]. PFAS have inimitable properties, which are ascribed to the bond between carbon and fluorine (C-F), which is strongly polarized in nature with a binding energy of 116 kcal/mol within the fluorinated chain [2, 3]. The stable C-F bond has cemented PFAS utilization in various applications, viz., industrial detergents, fire-fighting foams, polymerization processes, as a key component in manufacturing versatile materials designed to repel both water and grease across various applications, coating agents, non-stick cookware, and food packaging [2-4]. Despite their impeccable industrial applications, PFAS have been considered pollutants of significant global environmental concern owing to their long-lasting presence in the environment. The high bioamplification factor ascribed to their strong protein affinity has contributed to PFAS toxic effects in humans, flora, and fauna. Due to their stability, PFAS have been identified in many ecosystem compartments globally, with perfluorooctanoic acid (PFOA) and perfluorooctane sulfonic acid (PFOS) having the highest frequency of detection among PFAS, as documented by Elanchezhiyan et al. [3]. The presence of PFAS in aquatic environments and their health hazards due to long-term contact with both PFOA and PFOS have been discussed in the literature [2, 5-10]. Owing to the reproductive toxicity, neurotoxicity, and immunotoxicity of PFOA and PFOS in human well-being, “developed countries like the United States of America, through its Environmental Protection Agency (EPA), have set a health advisory limit of 70 ng/L for PFOA and PFOS, either individually or in combination, in drinking water” [2, 3, 11].

Furthermore, Jian et al. [12] cited that “the 3M company, together with the EPA in the United States of America, announced the phase-out of products containing PFAS with C6 and more, aimed at eliminating long-chain PFAS”, which are very persistent and bio-accumulative. As a result, the urgent need arises to identify effective and eco-conscious solutions to mitigate PFOA and PFOS contamination in the drinking aquatic environment due to their frequent occurrence.

It is worth noting that various methods for eliminating PFAS from water sources have been explored in scientific

research, viz., advanced oxidation [13-15], electro-flotation [16, 17], nanofiltration, and membrane processes [18-20], chemical precipitation [21], biodegradation [22-24] as well as solid-liquid adsorption processes [3, 11]. The breakdown of PFAS, enabled through advanced oxidation or biological mechanisms, results in the formation of undesirable byproducts, such as the fluorine ion (F^-) and shorter-chain PFAS substances with greater potential risks and significantly harder to remove from an aqueous environment than the parent PFAS [25]. Similarly, the degradation of PFAS using advanced oxidation involves multiple chemical reactions catalyzed by hydroxyl radicals and sulfate radicals, which requires high energy usage to regenerate these radicals, thus rendering the process expensive for industrial application [25, 26]. Membrane processes have been validated as efficient in the elimination of PFAS from liquid solutions; however, this technology is associated with some drawbacks, such as membrane fouling, which can be minimized by incorporating a nanofiltration or reverse osmosis process, thus rendering the process expensive and energy-intensive [27]. Conventional biodegradation techniques have been shown to lack effectiveness in breaking down PFAS under ambient conditions [28]. However, recently reported literature [22-24, 28] suggests that there has been a breakthrough in the biodegradation of PFOA and PFOS using novel bacterial strains; however, these technologies are still at their infant stages for practical application. On the other hand, the adsorption process has exhibited strong effectiveness in eliminating PFOA and PFOS [25]. The application of conventional adsorbents in eliminating PFAS contaminants, including activated carbon, carbon nanotubes, polymeric resin, and zeolite, has been documented in the literature [28, 29]. However, the utilization of these adsorbents presents several drawbacks, such as limited availability, which may lead to resource depletion, non-biodegradability, high costs, and the possibility of generating secondary pollutants that may negatively impact the environment [30]. Therefore, this highlights the critical need for advancing cost-effective and environmentally friendly adsorbents for PFAS mitigation.

In recent years, research on cost-effective and eco-friendly adsorbents, particularly chitosan-based composites, for mitigating PFOA and PFOS from contaminated water has expanded significantly [3, 25, 28, 30, 31]. The increasing application of adsorbents derived from chitosan is because of its properties that are largely influenced by chitosan's abundant amino groups and both primary and secondary hydroxyl (-OH) groups incorporated within the framework of chitosan, making it an ideal site for binding specific compounds [3]. According to Elanchezhiyan, et al. [3], "chitosan is defined as a polymer composed of β(1 → 4) glucosamine and *N*-acetyl-D-glucosamine, which is derived from chitin through the process of *N*-deacetylation, which is the most abundant biopolymer after cellulose." Sourced from the exoskeletal remains of shellfish and marine arthropods like crabs and shrimps, as well as fungal mycelium chitin is converted to chitosan through deacetylation, offering significant benefits in environmental remediation applications [25]. It is worth noting that an adsorbent is deemed parsimony viable if the material can be easily prepared and applied with minimal energy consumption, is abundantly available in nature, and can generate no byproducts. Chitosan meets these requirements and is recognized as a cost-effective raw material for creating new adsorbents, as reported by Long et al. [25]. The increasing interest in chitosan-based adsorbents is also due to their inherent features, viz., outstanding biocompatibility, biological breakdown capability, bactericidal effects, non-toxic nature, flexibility for alterations, and the presence of various functional groups, as highlighted by Zakaria et al. [30]. It is important to highlight that chitosan hydrogels have gained popularity for their application in wastewater treatment processes. However, using pristine chitosan flakes or hydrogel beads presents certain limitations, including their rigidity, slow adsorption kinetics, and high solubility in acidic aqueous solutions [3]. The undesirable properties of pristine chitosan can be addressed by integrating carbon-based materials into the chitosan matrix, thereby improving its insolubility in mildly acidic aqueous solutions and boosting its adsorption efficiency [3, 32]. Despite the desirable properties of chitosan composites as adsorbents, studies on parametric optimization for the sorption of PFAS from aqueous environments are scant. Most studies reported in the literature are limited to adsorption kinetics; as such, there is a need to conduct studies focusing on process parametric optimization for effective process design.

Herein, the retention of PFOA and PFOS on chitosan-carbon nanotube (CCNT) hydrogel beads as a model adsorbent from an aqueous solution was investigated. Owing to their exceptional features, namely, high tensile strength, expansive surface area, and lightweight composition, carbon nanotubes (CNTs) have the potential to be excellent nanofillers for addressing the drawbacks of pure chitosan composites in water treatment applications. The scientific contribution of the present work processes parametric optimization, precisely the influence of solution pH, initial adsorbate concentration, adsorbent amount, and interaction time, examined through Central Composite Design (CCD) within Response Surface Methodology (RSM) as a first case.

2. Materials and Methods

2.1. Chemical Reagents

Chitosan powder derived from shrimp shells having a deacetylation degree of at least 75%, along with sodium hydroxide (NaOH) pellets (95% anhydrous basis), sodium chloride (NaCl), methanol (CH_3OH) (99.9% pure), 98% pure sulfuric acid (H_2SO_4), and glacial acetic acid ($C_2H_4O_2$) (99.7% pure) were provided by Sigma-Aldrich, South Africa. PFOA ($C_8HF_{15}O_2$), PFOS ($C_8HF_{17}O_3S$), and multiwall CNTs (>98% carbon basis) were provided by Lasec laboratories, Durban, South Africa.

2.2. Adsorbent Preparation

The CCNT hydrogel beads utilized in the present study were synthesized using multiwall CNTs modified with acid. Pristine CNTs naturally tend to group and stay closely bound when in a liquid solution. However, the effectiveness of using CNTs for water treatment relies heavily on the ability to separate them into individual nanotubes, ensuring homogeneity and stability, as reported by Sobczak-Kupiec et al. [33]. In this study, CNT modification involved "immersing a known quantity of CNTs in a solution of high concentration of H_2SO_4 and nitric acid with a volume ratio of 1:2 for 24 hours," as reported by Elanchezhiyan et al. [2].

An oxygen-rich acid solution enabled the bonding of functional groups, i.e., -COOH and -OH, to the exterior of the carbon nanotubes (CNTs), which are crucial for eliminating targeted contaminants from aqueous environments. Subsequently, the acid-functionalized CNTs are crucial for eliminating model contaminants in aqueous solutions. Following the acid treatment, ultrapure deionized water was used to rinse the CNTs until the filtrate's pH level reached 7, as measured by a HANNA HI 9825 pH meter. Additionally, it is crucial to note that altering the CNTs was necessary to attain a surface with greater hydrophilicity than the unmodified CNTs.

The preparation of CCNT hydrogel beads involved "dissolving 100 g of chitosan in a 400 mL solution of 1% v/v glacial acetic acid. Chitosan generally has poor solubility in water; however, it dissolves more effectively in mildly acidic environments. The chitosan and glacial acetic acid solution was vortexed at 200 rev/min with a magnetic stirrer at room temperature for 24 hours to ensure thorough dissolution, as chitosan's solubility is limited at room temperature, requiring prolonged vortexing. To minimize evaporation, the chitosan-CNT mixture was covered with aluminum foil during the vortexing process since glacial acetic acid is quite volatile. Subsequently, the chitosan-glacial acetic acid mixture was enhanced with 5 wt.% of functionalized CNTs relative to the amount of chitosan and then stirred at 200 rev/min for 2 hours. The objective was to achieve a uniform dispersion of CNTs within the mixture.

The dense CCNT mixture was then degassed in a vacuum desiccator until all air pockets vanished from the dense mixture. CCNT hydrogel beads were produced by gradually dripping the dense CCNT mixture into a solution consisting of 15 wt.% NaOH and 95 %v/v CH_3OH at a volume ratio 4:1, using a 10 mL syringe. The CCNT gel precipitated into CCNT beads and was allowed to soak in the NaOH-CH_3OH solution for 24 hours. Following that, CCNT beads were washed with deionized water until the filtrate reached a pH of 7 before being utilized for adsorption experiments. Utilizing the Fourier transform infrared spectrophotometer (FTIR, VERTEX 70), the existence of functional groups was analyzed, as discussed in previous works [32].

2.3. Batch Studies

Experiments for the retention of PFOA and PFOS on CCNT hydrogel beads were conducted at adsorbent and adsorbate loads starting from 0.05 g/L to 1.5 g/L and 5 mg/L to 20 mg/L, respectively, at a solution pH ranging from 4 to 7. The contact time ranged from 2 hours to 48 hours. Experiments were carried out using clear 50 mL containers equipped with threaded lids containing a sample volume of 50 mL for both PFOA and PFOS. The sample containers were positioned inside a shaking device, which was operated at a steady shaking rate of 150 rpm and a temperature of 293 K. "Subsequently, a specific sample volume was extracted, passed through a 0.45 µm syringe filter, and transferred into a 10 mL sample tube. The samples were centrifuged at 5000 rpm for 10 minutes" [32]. Following centrifugation, the supernatant solution was analyzed using high-pressure liquid chromatography-tandem mass spectrometry (HPLC-MS/MS). The effectiveness of eliminating model contaminants was assessed by measuring the difference between the initial and final concentrations in the aqueous solution, as described by equation (1).

$$Adsorption\ \% = \left[\frac{C_o - C_f}{C_o}\right] \times 100 \quad (1)$$

Where C_0 and C_f represent the initial and final concentrations of the adsorbates expressed in mg/L, respectively.

2.4. Parametric Optimization Studies Using RSM

Herein, the influence of the solution pH, adsorbate starting concentration, CCNT dose, and interaction time were investigated by using a standard central composite design (CCD) in RSM by adopting the procedure recommended by Karimifard and Moghaddam [34] in Design-Expert version 11. The CCD in the RSM framework is applied to model a quadratic surface by analyzing the interactions among chosen parameters and fine-tuning the conditions with a reduced number of experiments. Furthermore, "employing CCD allows for the evaluation of sensitive data for the purpose of addressing inadequacy without necessitating a substantial number of design points, thereby cementing its role in process optimization research" [32, 34, 35]. The parameters investigated for PFOA and PFOS enhancement of the removal models' efficiency are displayed in Table 1, showing the codes, ranges, and levels for each, i.e., low (-1) and high (+1).

Table 1. Experimental range and levels of independent process variables

Factor	Units	Code	Low -1	High +1
pH	--	A	4	10
Adsorbate Conc.	mg/L	B	5	20
Adsorbent	g/L	C	0.05	1.5
Time	h	D	2	48

To conduct statistical analysis, the relationship between the system's response and the independent variables was estimated using equation (2) in the context of RSM, with all process variables designated as X_i (3).

$$Y = \beta_0 + \sum_{i=1}^{k} \beta_i X_i + \sum_{i=1}^{k} \beta_{ii} X_i^2 + \sum_{i=1}^{k=1} \sum_{j=i+1}^{k} \beta_{ij} X_i X_j + \varepsilon \quad (2)$$

$$X_i = \left(\frac{z_i - z_0}{\Delta z_i}\right) \beta_d \quad (3)$$

The predicted response, Y, "is determined using input variables X_i and X_j, along with the regression constants β_0, β_i, β_{ii}, and β_{ij}, which relate to the intercept, linear coefficient, quadratic coefficient, and regression coefficient, respectively" [35]. The study focuses on analyzing and optimizing the number of factors k, while also considering the random error, ε; the variable. z_i indicates the coded value of the ith independent variable, whereas z_0 represents the uncoded value. According to Garg et al. [1], "the variable β_d represents the primary coded limit value within the matrix for each variable while Δz_i signifies the step-change codification of the value between the low level (-1) and high level (+1)." The purpose of codifying independent variables was exclusively to ensure their standardization, as these variables can differ in both measurement units and scales of magnitude. This codification process was employed to ensure that all independent variables have an equal impact on the specified responses. The precision and dependability of the fitted models were assessed through analysis of variance (ANOVA), which compared the variability due to changes in the combinations of variable levels against the variability resulting from random measurement errors in the generated responses [36]. Consequently, performing this comparison facilitated the evaluation of the significance of the regression in predicting the resulting output while considering the origins of variability in the experiment.

3. Results and Discussion

3.1. Adsorbent Characterization

In this study, FTIR spectra were utilized to examine the alterations in oscillations of functional groups within the adsorbent, observed both prior to and following the adsorption process. FTIR analyses were conducted at a wavenumber range of 500 cm^{-1} to 4000 $cm^{-1,}$ and the findings are shown in Figure 1. According to Elanchezhiyan et al. [3], "for the CCNTs adsorbent, the weak absorption peak at 3297 cm^{-1} is ascribed to the -OH and -NH_2 stretching vibrations of the polysaccharide within the chitosan structure. The bend at 3436 cm^{-1} can be assigned to the -OH functional group resulting from incorporating CNTs. The absorption peaks at 1664 cm^{-1} and 1593 cm^{-1} are attributed to the presence of C=O and -N-H stretching vibrations, respectively, confirming the presence of the chitin moiety, i.e., -$NHCOCH_3$ in chitosan as a result of using partially deacetylated chitosan flakes. The peak at 2884 cm^{-1} can be attributed to the -CH stretching vibration of the chitosan polymer". The 1028 cm-1, 1387 cm-1, and 1431 cm^{-1} peaks can be assigned to the -C-O-C stretching vibration, -CH group deformation, and -CN stretching vibration, respectively [37]. The peaks at 2919 cm^{-1} and 2848 cm^{-1} are attributed to asymmetric CH_2 stretching vibrations of the CNTs; the peak at 1630 cm^{-1} is assigned to the CNTs' conjugated C=C stretching vibrations. Moreover, the weak peak at 1226 cm^{-1} and 1573 cm^{-1} corresponds to C-O-H bending and C=C alkene stretching vibrations from the CNTs, respectively. The string peaks at 1035 cm^{-1} are assigned to the C-H in-plane bending on the CNTs surface, as discussed by Karimifard and Moghaddam [34]. The strong peaks on the functional groups on the surface of CCNTs are attributed to the acid functionalization of CNTs, leading to the release of carbon at the defective sites and end points of the CNTs. The strength of the bands reflects the effective integration of the targeted functional groups, thereby improving the effectiveness of the model adsorbent in capturing contaminants. From the FTIR results, it is apparent that there were changes in the element content as demonstrated by the band intensity changes, explicitly indicating the uptake of PFOA and PFOS on CCNT hydrogel beads.

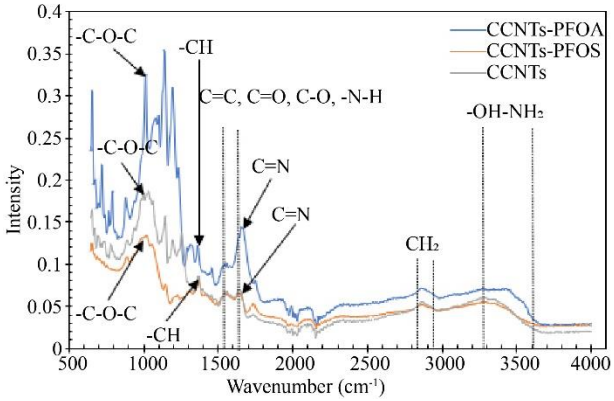

Fig. 1 FTIR spectra of CCNTs, CCNTs-PFOA, and CCNTs-PFOS

3.2. Parametric Optimization Using CCD in RSM Development of a Regression Model in RSM

Herein, second-order quadratic regression models were developed to align with the observed responses (i.e., PFOA (Y_1) and PFOS (Y_2) percentage removal) by examining the correlation between dependent and independent variables, as outlined in the coded equations (4) and (5), respectively.

$$Y_1 = 76.27 - 3.50A - 8.89B + 7.72C + 22.50D - 4.12BC - 6.25BD + 5.25CD - 15.11C^2 - 29.11D^2 \quad (4)$$

$$Y_2 = 81.70 - 2.78A - 9.22B + 7.83C + 22.72D - 4.192BC - 6.06BD + 5.06CD - 6.85A^2 - 8.35C^2 - 29.35D^2 \quad (5)$$

Through coefficient analysis, Equations (4) and (5) enable the identification of the relative effects of terms and their interactions [38]. For the coded equations developed in RSM, a higher absolute coefficient value indicates a greater influence of the respective term. Equations (4) and (5) suggest

that it can be deduced that factor A (pH) had the least absolute values, suggesting the least impact it has on the removal of PFOA and PFOS from an aqueous phase when compared to the other factors, i.e., B (initial adsorbate concentration), C (adsorbent dose), and D (interaction time). On the other hand, based on the absolute values, it is apparent that the term D^2 exerted the greatest influence on PFOA and PFOS adsorption behaviour. The significance of the models and the interactions between the independent variables underwent additional assessment through analysis of variance (ANOVA) and model fit statistics, as presented in Tables 2 and 3.

Table 2. ANOVA and fit statistics of the PFOA removal predictive model

Source	Sum of Squares	df	Mean Square	F-value	p-value	
Model	25489.58	9	2832.18	85.53	< 0.0001	significant
A-pH	220.50	1	220.50	6.66	0.0179	
B-PFOA Conc.	1422.22	1	1422.22	42.95	< 0.0001	
C-CCNT dose	1073.39	1	1073.39	32.41	< 0.0001	
D-Time	9112.50	1	9112.50	275.18	< 0.0001	
BC	272.25	1	272.25	8.22	0.0095	
BD	625.00	1	625.00	18.87	0.0003	
CD	441.00	1	441.00	13.32	0.0016	
C^2	786.71	1	786.71	23.76	< 0.0001	
D^2	2919.38	1	2919.38	88.16	< 0.0001	
Residual	662.29	20	33.11			
Cor Total	26151.87	29				
Fit statistics of the quadratic model						
Std. Dev.	R^2	Adjusted R^2		Predicted R^2	Adeq. Precision	
5.75	0.9747	0.9633		0.9358	26.6460	

Table 3. ANOVA and fit statistics of the PFOS removal predictive model

Source	Sum of Squares	df	Mean Square	F-value	p-value	
Model	25626.51	10	2562.65	80.29	< 0.0001	significant
A-pH	138.89	1	138.89	4.35	0.0507	
B-PFOS Conc.	1530.89	1	1530.89	47.96	< 0.0001	
C-CCNT dose	1104.50	1	1104.50	34.60	< 0.0001	
D-Time	9293.39	1	9293.39	291.16	< 0.0001	
BC	280.56	1	280.56	8.79	0.0080	
BD	588.06	1	588.06	18.42	0.0004	
CD	410.06	1	410.06	12.85	0.0020	
A^2	133.29	1	133.29	4.18	0.0551	
C^2	198.03	1	198.03	6.20	0.0222	
D^2	2445.71	1	2445.71	76.62	< 0.0001	
Residual	606.46	19	31.92			
Cor Total	26232.97	29				
Fit statistics of the quadratic model						
Std. Dev.	R^2	Adjusted R^2		Predicted R^2	Adeq. Precision	
5.65	0.9769	0.9647		0.9258	25.7068	

Generally, the sum of squares value can be utilized to analyze the significance of any process-related parameter. Within the ANOVA framework, a large sum of squares signifies a significant influence of the respective variable. It can be inferred from Tables 2 and 3 that for the current work, the significance of individual parameters was in the order of interaction time (D) > adsorbate initial concentration (B) > adsorbent dose (C) > solution pH (A). The results indicate that in the adsorption of PFOA and PFOS from the aqueous phase, contact time played a crucial role in determining their uptake, whereas solution pH exhibited a relatively minor influence in comparison to other factors, namely B, C, and D. The relatively low sum of squares recorded for the solution pH does not imply that this parameter had an insignificant effect in the uptake of the model adsorbates. The ANOVA results in terms of the significance of individual parameters are

congruent to the physical meaning of the predictive coded models, i.e., Equation (4) and Equation (5) built-in RSM.

The significance of the quadratic model was evaluated by analyzing its F-value, which needed to surpass those of other parameters, and its p-value, a probability indicator that was required to stay below 0.05, as recommended by Alimohammadi et al. [39]. From Tables 2 and 3, it can be observed that both the PFOA and PFOS-coded predictive models recorded F-values of 85.53 and 80.29, respectively, and p-values of less than 0.0001. The F-values of the predictive models obtained for the sorption of both PFOA and PFOS demonstrate the relevance and validity of the models, indicating only a 0.01% probability that such large F-values might result from interference or background disturbances. Furthermore, the p-values of the models, being less than 0.05, indicate that all terms within the model hold statistical relevance. In the case of PFOA and PFOS predictive models, i.e., Equation (4) and Equation (5), respectively, all model terms are significant with p-values of less than 0.05 except for A and A^2 having p-values of 0.0507 and 0.0551, respectively (see Table 3). The slightly high p-values suggest that terms A and A^2 are the least significant terms in the model, i.e., equation (5). However, it is worth noting that exclusively model parameters associated with p-values greater than 0.100 imply not being significant within the framework of RSM; as such, the model does not require any reduction when considering model terms with a p-value of 0.100 or less.

The goodness of fit for the quadratic PFOA and PFOS removal predictive models was assessed by applying the model fit statistics within ANOVA, as depicted in Tables 2 and 3, respectively. The evaluation of the models' significance was conducted using key metrics such as the coefficient of determination (R^2), adjusted R^2, adequate precision, and standard deviation (Std. Dev). In ANOVA, the R^2 parameter measures the extent of variation in predicted values relative to the mean. Consequently, a model demonstrates strong predictive accuracy when the R^2 value approaches 1 [40]. Therefore, the R^2 values of 0.9747 and 0.9769 for the PFOA and PFOS systems, respectively, suggest that the developed predictive models can satisfactorily predict the removal efficiencies for the model adsorbates from solution at a Std. Dev. of ±5.75% (PFOA) and ±5.65% (PFOS). The models' goodness of fit was further evaluated by incorporating the adjusted R^2 value as a statistical metric that accounts for the quantity of samples analyzed and the total count of terms incorporated within the models [39, 40]. Notably, a greater number of variables in the model leads to a higher R^2 value, irrespective of whether the variable is significant, while the adjusted R^2 values do not increase with adding more variables, remaining lower than the R^2 value. From the fit statistics in Table 2 and Table 3, both the PFOA and PFOS systems reported high adjusted R^2 values greater than 0.96 but remained less than the reported R^2 values, suggesting that the developed models satisfactorily predict the desired responses with minimal deviation. On the other hand, the variation of less than 0.2 between the adjusted R^2 and predicted R^2 for both systems under investigation is evidence that the predicted R^2 aligns with the adjusted R^2. Moreover, from the ANOVA results, it is apparent that the developed models have an adequate ratio of greater than 4, implying an adequate signal. The adequate precision quantifies the signal-to-noise ratio; therefore, the obtained ratios of greater than 4 suggest that the constructed models facilitate the exploration of the design space.

3.2.1. Model Validation

Herein, the quadratic models developed were validated by analyzing the graphs of the percentage removal of PFOA and PFOS predicted by the model against the actual percentage removal of PFOA and PFOS, as presented in Figure 2. Additionally, a diagnostic test was performed by plotting the externally studentized results against the experimental runs (see Figure 3).

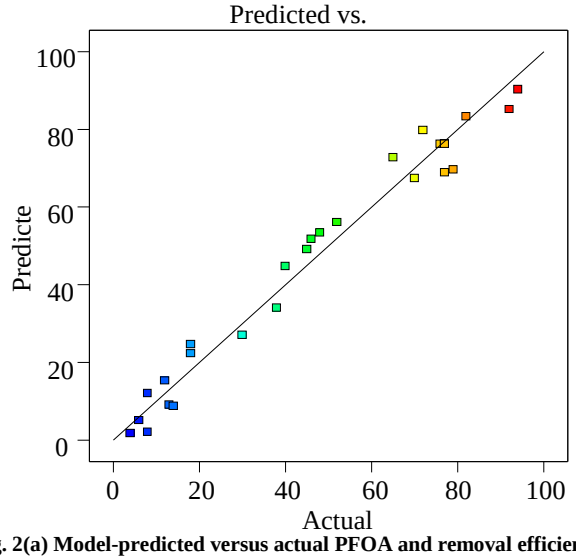

Fig. 2(a) Model-predicted versus actual PFOA and removal efficiency

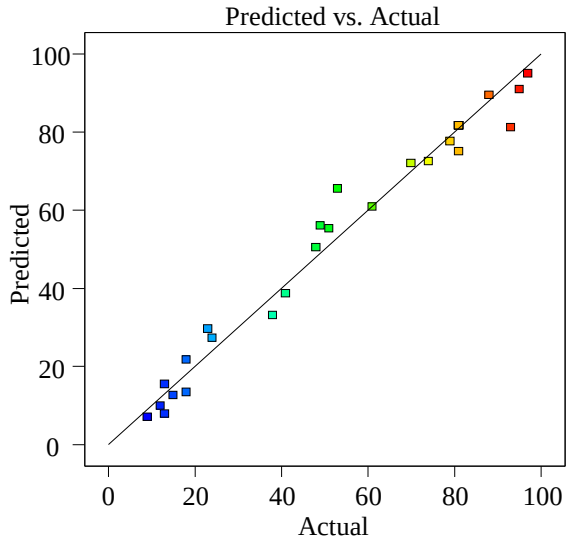

Fig. 2(b) Model-predicted versus actual PFOS and removal efficiency

According to Montgomery [40], an effective prediction can be illustrated by the plot that compares predicted responses to actual values, which should show a random distribution near the 45° line (see Figure 2). Data points evenly distributed above or below the 45° line indicate regions of overestimation and underestimation, respectively. In this study, Figure 2 reveals that the data points for both the PFOA and PFOS systems are largely concentrated near the diagonal line at a 45° angle, indicating a strong relationship among the distinct, independent variables (such as solution pH, initial adsorbate concentrations, CCNT dose, and interaction duration) and the responses (i.e., PFOA and PFOS percentage removals). The pattern observed in Figure 2 is attributed to the relatively high predicted R^2 values of 0.9358 for PFOA and 0.9258 for PFOS, indicating a good model fit. Therefore, the models show negligible errors within the specified operational parameters.

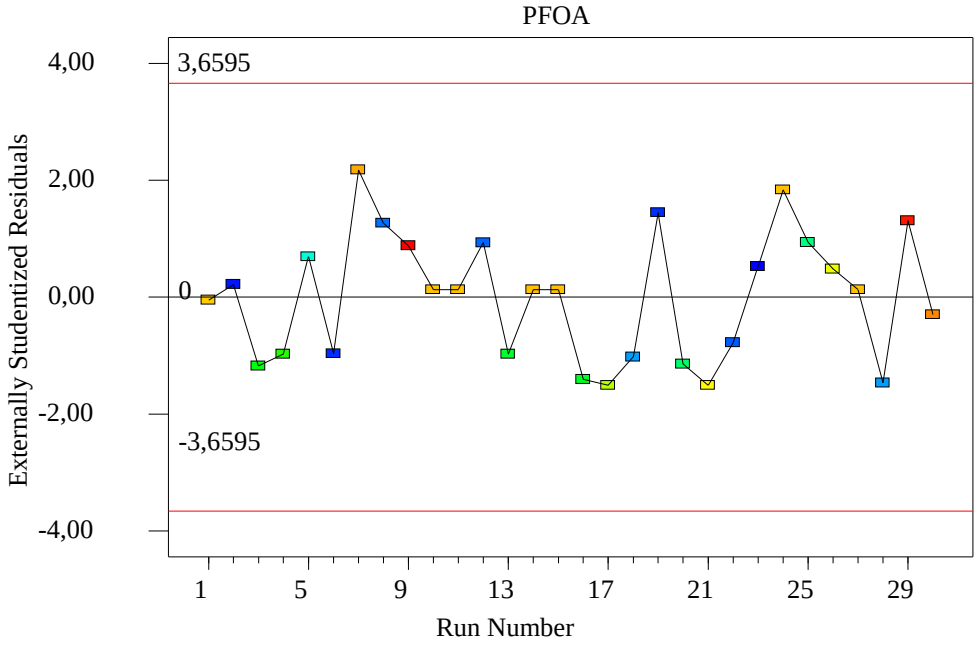

Fig. 3(a) Externally studentized residuals versus run number for PFOA adsorption system

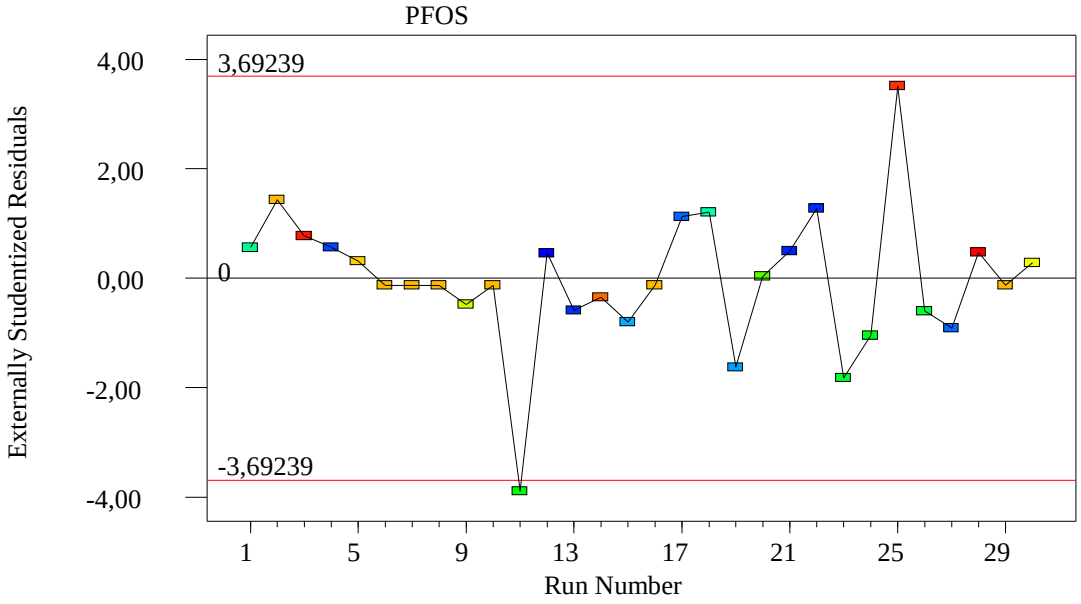

Fig. 3(b) Externally studentized residuals versus run number for PFOS adsorption system

The diagnostic plots illustrating externally studentized residuals against experimental runs for PFOA and PFOS adsorption systems, as depicted in Figure 3, were utilized to investigate any hidden variables that might have impacted the experimental responses. Statistically speaking, a model is considered to have strong predictive capability if the externally studentized residuals plotted against experimental runs show a random distribution without any discernible pattern, which is indeed the case in this study (see Figure 3). Conversely, the presence of a pattern suggests that a time-related factor may be influencing the results. Studentized residuals aid in evaluating the discrepancies between actual and forecasted target outcomes within a standard regression model while accounting for fluctuations among various predictor variables. Specifically, in this study, an externally studentized residual that exceeds 4 is classified as an "outlier." An "outlier," or a data point with significant leverage, can potentially distort the fitted model, resulting in biased outcomes. Therefore, no outliers were detected for the quadratic models designed to analyze the uptake of PFOA and PFOS on CCNT hydrogel beads. All externally studentized residuals remained within permissible bounds, confirming that no transformations were necessary for the percentage removal rates of PFOA and PFOS [40].

3.2.2. Evaluation of the Single-Factor Effect on PFOA and PFOS Removal

Herein, the influence of single factors, i.e., pH, adsorbate concentration, CCNT dose, and interaction time on the responses of PFOA and PFOS removal efficiencies were analyzed using the XY plots (see Figure 4 and Figure 5) based on the predictive models developed in RSM.

3.2.3. Effect of Solution pH

In any typical adsorption process, the pH of the solution serves a crucial function as it influences the ionization level of the model adsorbates [3]. Moreover, variations in solution pH can influence the surface charge of the model adsorbent. The influence of solution pH on the sorption of PFOA and PFOS on CCNT was investigated for a pH range of 4 to 10, and the findings are presented in Figure 4. From Figure 4, it can be inferred that an increase in pH from 4 to 10 resulted in a decrease in the percentage removal of PFOA and PFOS, implying the dependence of the adsorption process on pH. The highest percentage removals of greater than 80% for PFOA as well as PFOS were recorded for a solution pH of 4, suggesting that the adsorbent (i.e., CCNT hydrogel beads) functional groups were protonated under an acidic environment, enabling CCNT hydrogel beads to effectively capture the negatively charged PFOA and PFOS via robust electrostatic forces. The reported acid dissociation constants (pKa) for PFOA and PFOS in the literature are 2.8 and -3.27, respectively [41], which is lower than the pH range of 4 – 10 adopted in this research, allowing PFOA and PFOS to exist in deprotonated forms. Conversely, the determined point of zero charge (pHpzc) for CCNT is 8.5, signifying that at solution pH levels below this value, the CCNT surface possesses a positive charge. As such, the observed gradual decrease in PFOA and PFOS removal efficiency with an increase in pH can be attributed to the reduction in the number of positive sites on the CCNT surface, thus compromising the uptake of PFOA and PFOS by electrostatic forces.

Additionally, CCNT possesses a range of functional groups, including carboxyl, amino, and hydroxyl, which easily establish a structure engaging with anionic PFOA and PFOS through electrostatic forces under acidic conditions [3]. It is crucial to recognize that the results of the present study align with the findings reported by Wang and Shih [41] on the sorption of PFAS on alumina and Elanchezhiyan et al. [3] on the sorption of PFAS on “reduced graphene oxide-modified zinc ferrite immobilized chitosan beads.” Therefore, the observed trend may indicate the presence of a distinct chemical interaction between sulfonate and the CCNT surface, considering that both PFOA and PFOS were likely affected by identical electrostatic forces.

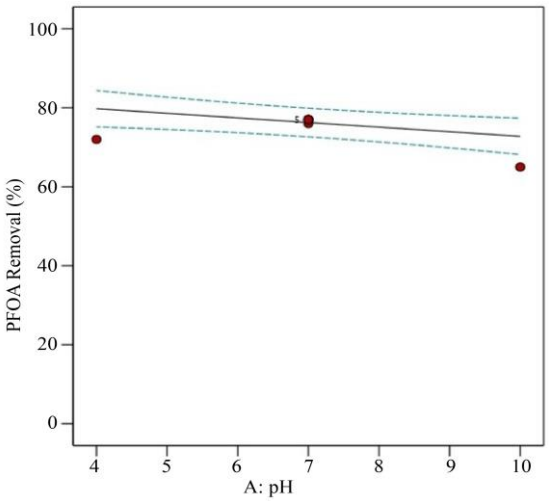

Fig. 4(a) XY plots for the effect of pH on PFOA percentage removal

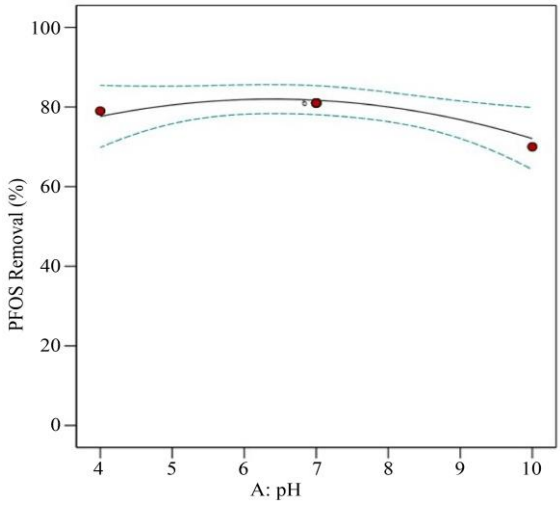

Fig. 4(b) XY plots for the effect of pH on PFOS percentage removal

3.2.4. Adsorbate Initial Concentration

The results of this study regarding the impact of initial adsorbate concentration on the percentage removal of PFOA and PFOS are illustrated in Figure 5. It is apparent from Figure 5 that a rise in the initial adsorbate concentration led to a steady decline in the percentage removal of PFOA and PFOS. The observed trend can be attributed to the fundamental principle that, at higher concentrations, the ratio of adsorbate molecules to available adsorption sites increases significantly.

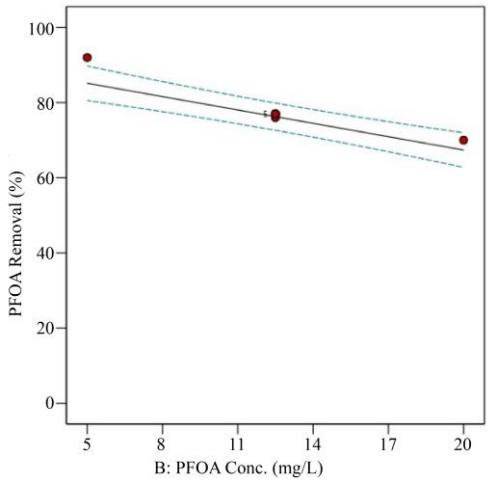

Fig. 5(a) XY plots for the effect of adsorbate initial concentration on PFOA percentage removal

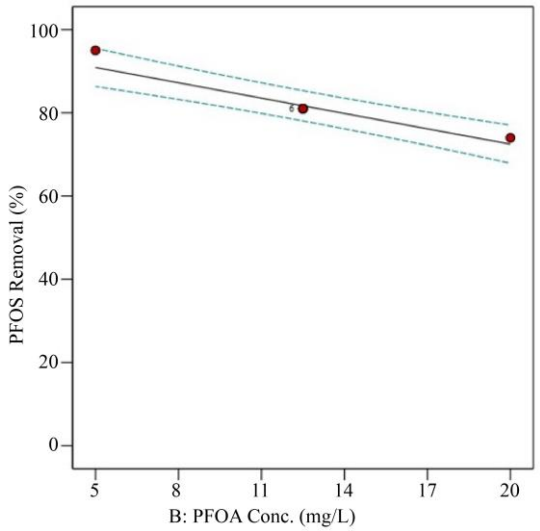

Fig. 5(b) XY plots for the effect of adsorbate initial concentration on PFOS percentage removal

Consequently, the maximum removal efficiencies for both PFOA and PFOS were achieved at an initial adsorbate concentration of 5 mg/L, owing to the substantial availability of adsorption sites in relation to the adsorbent's surface area, where the adsorbate molecules are accommodated. Moreover, it is apparent that the model adsorbent demonstrated a higher affinity for PFOS as compared to PFOA, which is ascribed to the higher hydrophobic nature of PFOS in contrast to PFOA, suggesting that the uptake of PFOS on CCNT hydrogel beads is through hydrophobic interactions and electrostatic attraction [28].

3.2.5. Adsorbent Dose

Figure 6 suggests that the efficiency of PFOA and PFOS elimination, expressed as a percentage, improved as the CCNT hydrogel beads dosage increased within the range of 0.05 g/L to 1.5 g/L. Similarly, the observed trend can be explained by the fundamental principle that increasing the quantity of adsorbent results in a greater adsorption surface area, thereby enhancing the availability of active sites for the adsorption of the target adsorbates. It can be inferred from Figure 6 that the maximum sorption of PFOA and PFOS was attained at a CCNT dosage of 1.5 g/L for both compounds. It is important to mention that an increase in adsorbent dose above 0.775 g/L did not result in a rapid percentage uptake of PFOA and PFOS on CCNT at a fixed adsorbate concentration.

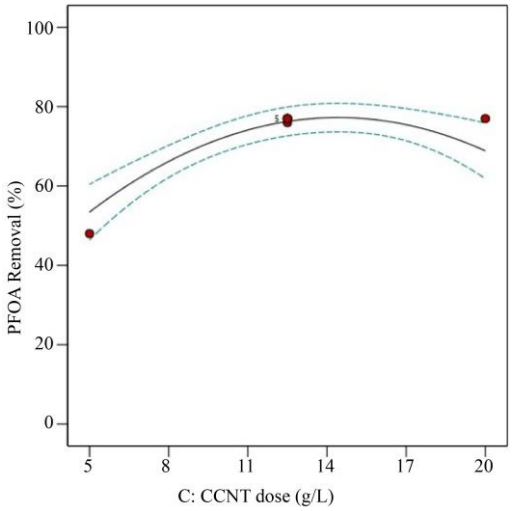

Fig. 6(a) XY plots for the effect of adsorbent dose on PFOA percentage removal

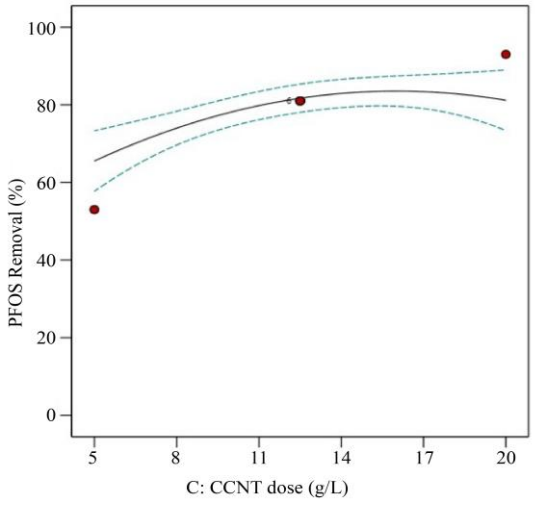

Fig. 6(b) XY plots for the effect of adsorbent dose on PFOA percentage removal

The plateau observed in PFOA and PFOS removal with increasing CCNT doses above 0.775 g/L indicates that further increases had a negligible impact on PFOA removal efficiency beyond this adsorbent dose. However, the uptake of PFOS improved by 10% when the adsorbent dose varied within the range of 0.775 g/L to 1.5 g/L.

3.2.6. Contact Time

The influence of contact time on the percentage removal of PFOA and PFOS from the aqueous phase was examined across a duration spanning 2 to 48 hours, as illustrated in Figure 7. The findings of this study indicate a significant enhancement in the removal efficiency of PFOA and PFOS as contact time was extended.

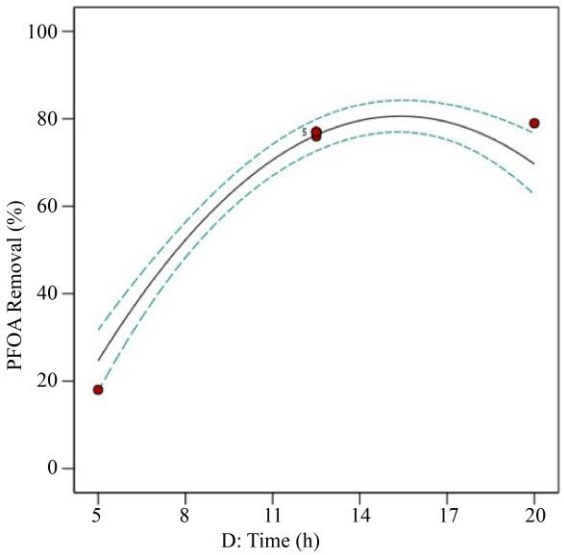

Fig. 7(a) XY plots for the effect of contact time on PFOA percentage removal

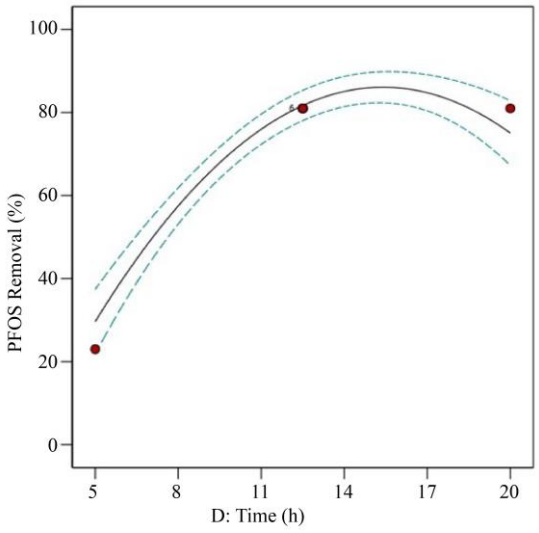

Fig. 7(b) XY plots for the effect of contact time on PFOS percentage removal

In a standard adsorption process, the observed pattern is due to the increasing adsorption rate as contact time extends, which results from the presence of unoccupied adsorption sites ready for adsorbate interaction on the model adsorbent's exterior. It is essential to acknowledge that, after a certain period, a reduction in the adsorption rate was anticipated due to the limited availability of active sites on the adsorbent's surface.

Thus, the results of this study regarding contact time indicate that for the examined system, a high composition of CCNT active sites was occupied by PFOA and PFOS at a contact time of 25 hours.

A decline in the percentage removal rate of PFOA and PFOS was observed after 25 hours, which is evident from the relatively low percentage removals between 25 hours and 48 hours of contact time as depicted in Figure 7.

3.2.7. Evaluating the Effect of Interactive Factors on PFOA and PFOS Removal

The combined effect of independent variables, including contact time, CCNT, and adsorbate concentration, on the removal efficiency of PFOA and PFOS was evaluated using 3D response surface plots within the response surface methodology (RSM), as depicted in Figure 8.

Additionally, the study's findings on the interactive influence of contact time and adsorbent dosage on PFOA and PFOS removal are illustrated in Figure 8(a), covering a time span of 2 to 48 hours and a CCNT dose range of 0.05 to 1.5 g/L.

The results of the current study indicate a strong relationship between the initial adsorbate concentration (i.e., PFOA and PFOS) and adsorbent dose, such that an increase in CCNT dose and contact time results in an increase in PFOA and PFOS removal.

The highest PFOA and PFOS removals were recorded for a CCNT dose of 1.5 g/L at a contact time of 48 hours. Similarly, with the 3D surface plots, there was a minimal improvement in the uptake of PFOA and PFOS post a contact time of 25 hours.

This is evident from Figure 8(a), in which the 3D plots formed almost a plateau beyond a contact time of 25 hours, indicating a slow PFOA and PFOS uptake rate.

Furthermore, the curved edges of the 3D surface plots suggest that extending the contact time and increasing the adsorbent dose enhance the percentage removal of PFOA and PFOS. This observation confirms the substantial interaction effects between these two variables in the adsorption efficiency of the model adsorbates.

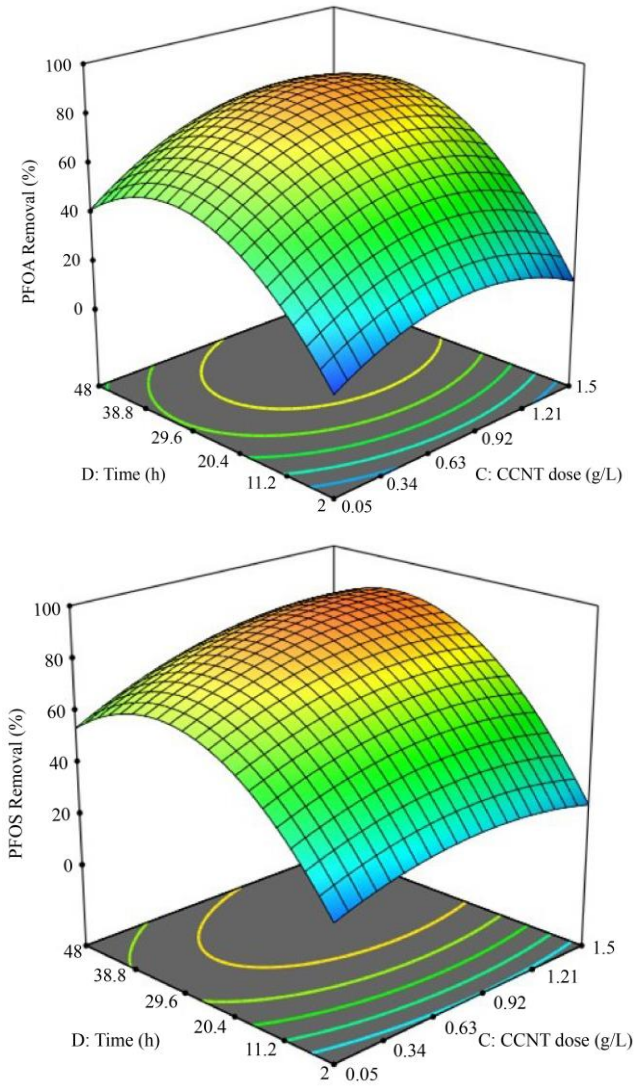

Fig. 8(a) 3D surface plots for the interactions between time and CCNT on PFOA and PFOS removal

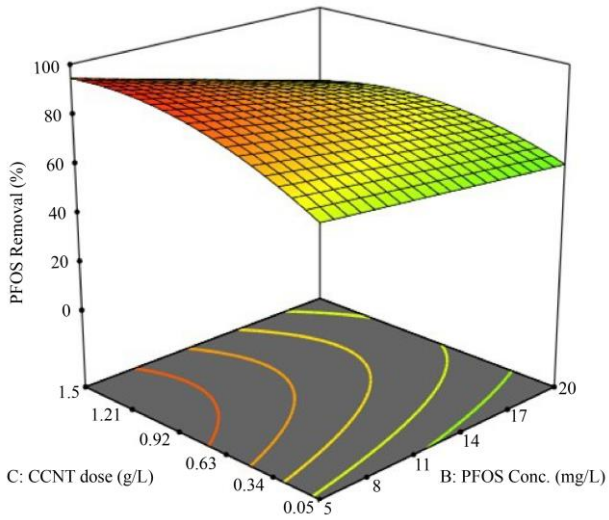

Fig. 8(b) 3D surface plots for the interactions between CCNT dose and adsorbate concentration on PFOA and PFOS removal

Figures 8(b) illustrate the interactive influence of CCNT and initial adsorbate concentration on the percentage removal of PFOA and PFOS. According to the ANOVA results presented in Tables 2 and 3, the interaction between CCNT and adsorbate concentration yielded p-values of 0.0095 for PFOA and 0.0080 for PFOS. These values indicate a comparatively lower significance in interaction effects than those observed between time and CCNT, as well as time and initial adsorbate concentration. This is evident from the 3D plots in Figure 8(b), an increase in PFOA or PFOS initial concentration from 5 mg/L to 20 mg/L with an increase in CCNT dosage did not have a significant effect on the percentage removal of PFOA or PFOS which is indicated by the flat surface of the 3D plots as presented in Figure 8(b). On the other hand, there was a gradual increase in PFOA and PFOS removal with an increase in CCNT dose from 0.05 g/L to 1.5 g/L at a constant adsorbate concentration of 5 mg/L**.**

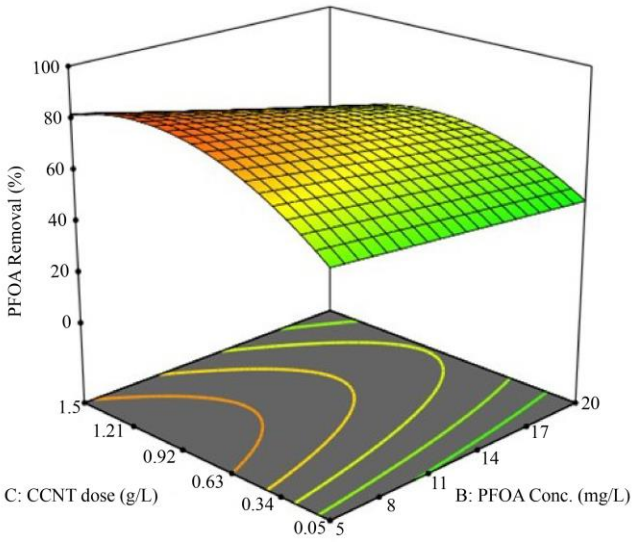

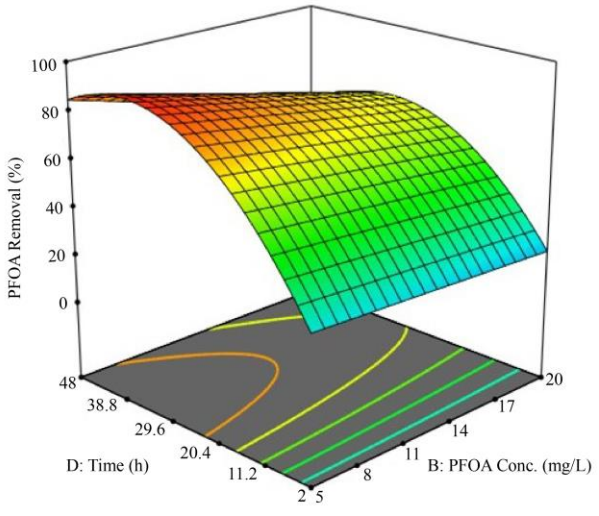

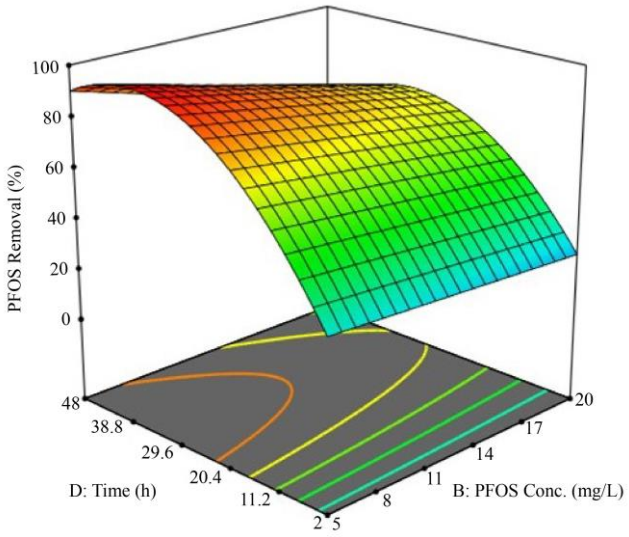

Fig. 8(c) 3D surface plots for the interactions between time and adsorbate concentration on PFOA and PFOS removal

Similarly, it is apparent from Figure 8(c) that for a concentration of the adsorbate at 5 mg/L, there was a significant uptake in PFOA and PFOS with an increase in contact time of up to 25 hours. After 25 hours of contact time, no significant uptake of PFOA or PFOS was observed, as indicated by the plateaus in Figure 8(c).

The trend observed in the 3D plots regarding the interaction between contact time and initial adsorbate concentration is substantiated by the recorded p-values of 0.0003 for PFOA and 0.0004 for PFOS. These values indicate a significant interaction effect between contact time and adsorbate concentration, strongly influencing the uptake of PFOA and PFOS onto CCNT hydrogel beads.

Based on Figure 8 and the ANOVA results presented in Tables 2 and 3, it can be concluded that the interactions among contact time, CCNT dosage, and initial adsorbate concentration had a significant impact on the removal efficiency of PFOA and PFOS by CCNT from the solution.

3.2.8. Optimization of PFOA and PFOS Adsorption on CCNT Hydrogel Beads

Optimization studies were conducted to identify the optimal conditions for maximizing the removal efficiency of PFOA and PFOS from an aqueous solution using the adsorbent. Herein, the developed quadratic models (i.e., Equation (4) and Equation (5)) in RSM were employed to identify the optimal levels of each factor (i.e., pH, adsorbate initial concentration, CCNT dose, and contact time) for the maximum uptake of PFOA and PFOS as depicted in Figure 9.

RSM provided 100 potential solutions, each with a desirability of 100% at a confidence level of 95%. The desirability function in RSM was utilized under the premise that if any of the four input variables in the adsorption process falls outside the desirable range, the quality of the responses is deemed completely unacceptable. "The desirability function facilitates the determination of operating conditions that satisfy all specified criteria for the responses while achieving the optimal balance in the combined response value", as explained by Candioti et al. [42]. To optimize the sorption of PFOA and PFOS on CCNT hydrogel beads, a single composite response was formed by integrating multiple responses, followed by optimization using RSM [42].

In the framework of RSM, a separate desirability function was developed for each response based on the fitted models, thereby defining the standards for optimization. It is important to mention that the desirability function ranges from 0 (unfavorable response) to 1 (fully favorable response). Intermediate values of desirability may reflect varying degrees of preference for the responses.

The optimal input factor levels needed to maximize the adsorption of PFOA and PFOS are illustrated in the ramp plots shown in Figures 9(a) and 9(b). Moreover, the desirability results obtained indicate that all input factors and the responses concerning the uptake of PFOA and PFOS achieved a complete desirability score of 1, leading to a perfect overall desirability score of 1.

Experiments for model validation were performed under ideal conditions as depicted in the ramp plots in Figure 9. Validation experiments recorded relatively high percentage removals of more than 90% and a standard deviation of ±1% for both PFOA and PFOS. The results obtained indicate that the developed predictive models, i.e., Equations (4) and (5), can be utilized to explore the design space with minimal inaccuracies.

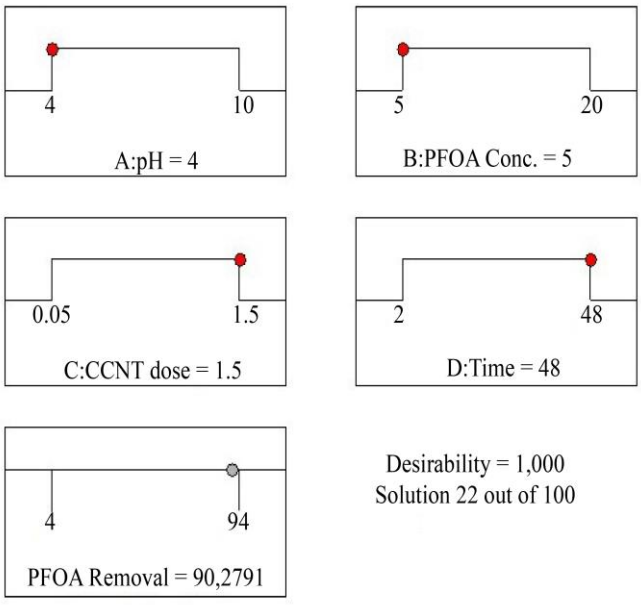

Fig. 9(a) Desirability ramp plots for the maximum removal of PFOA

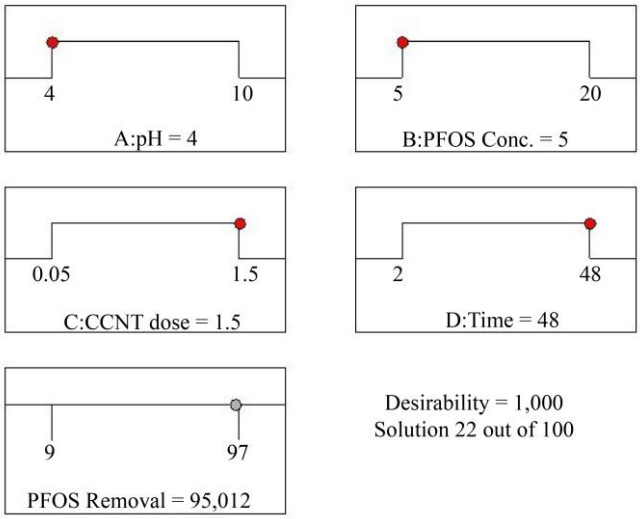

Fig. 9(b) Desirability ramp plots for the maximum removal of PFOS

4. Conclusion

The single adsorption experimental data explicitly indicate that the synthesized CCNT hydrogel beads demonstrated high affinity towards PFOS and PFOA, achieving more than 90% percentage removals under optimized conditions. The findings of this study identified optimal operating conditions for PFOA and PFOS removal, including a contact time of 48 hours, a solution pH of 4, an initial adsorbate concentration of 5 mg/L, and an adsorbent dosage of 1.5 mg/L, achieving a contaminant removal efficiency of at least 90% with a standard deviation below 1%. Furthermore, the response surface methodology (RSM) analysis clearly demonstrated that the adsorption of PFOA and PFOS onto the adsorbent was significantly influenced by the initial concentration of the model adsorbates, with higher initial concentrations leading to a reduced percentage removal rate. The results of this study suggest that the adsorption process occurred predominantly through physical adsorption, with pore-filling serving as the primary mechanism. It is essential to emphasize that this current study does not explicitly address the uptake mechanism of the model adsorbates. Although the model adsorbent exhibits a strong affinity for PFOA and PFOS under the specified optimal conditions, further research is required to optimise the temperature using RSM. Moreover, there is a scarcity of literature studies that report on evaluating the technical and economic aspects of chitosan-based adsorbents for industrial water treatment applications.

Acknowledgements

"Support by the Green Engineering Research Group at the Durban University of Technology in South Africa and the Environmental Pollution and Remediation Research Group at the Mangosuthu University of Technology in South Africa is greatly acknowledged."

References

[1] Shafali Garg et al., "Remediation of Water from Per-/Poly-Fluoroalkyl Substances (PFAS)–Challenges and Perspectives," *Journal of Environmental Chemical Engineering*, vol. 9, no. 4, 2021. [CrossRef] [Google Scholar] [Publisher Link]

[2] Siphesihle Mangena Khumalo, Babatunde Femi Bakare, and Sudesh Rathilal, "The Occurrence and Bioremediation of Emerging Polyfluorinated Compounds in Water Bodies: A Mini Review," *Applied Sciences*, vol. 12, no. 23, pp. 1-12, 2022. [CrossRef] [Google Scholar] [Publisher Link]

[3] S.SD. Elanchezhiyan et al., "Synthesis of Magnetic Chitosan Biopolymeric Spheres and their Adsorption Performances for PFOA and PFOS from Aqueous Environment," *Carbohydrate Polymers*, vol. 267, 2021. [CrossRef] [Google Scholar] [Publisher Link]

[4] Matthias Kotthoff et al., "Perfluoroalkyl and Polyfluoroalkyl Substances in Consumer Products," *Environmental Science and Pollution Research*, vol. 22, pp. 14546-14559, 2015. [CrossRef] [Google Scholar] [Publisher Link]

[5] Lin Cui et al., "Studies on the Toxicological Effects of PFOA and PFOS on Rats Using Histological Observation and Chemical Analysis," *Archives of Environmental Contamination and Toxicology*, vol. 56, pp. 338-349, 2009. [CrossRef] [Google Scholar] [Publisher Link]

[6] Pheruza Tarapore, and Bin Ouyang, "Perfluoroalkyl Chemicals and Male Reproductive Health: Do PFOA and PFOS Increase Risk for Male Infertility?," *International Journal of Environmental Research and Public Health*, vol. 18, no. 7, pp. 1-20, 2021. [CrossRef] [Google Scholar] [Publisher Link]

[7] Shuyu Liu, Nuoya Yin, and Francesco Faiola, "PFOA and PFOS Disrupt the Generation of Human Pancreatic Progenitor Cells," *Environmental Science & Technology Letters*, vol. 5, no. 5, pp. 237-242, 2018. [CrossRef] [Google Scholar] [Publisher Link]

[8] Shuji Tsuda, "Differential Toxicity between Perfluorooctane Sulfonate (PFOS) and Perfluorooctanoic Acid (PFOA)," *The Journal of Toxicological Sciences*, vol. 41, pp. SP27-SP36, 2016. [CrossRef] [Google Scholar] [Publisher Link]

[9] Kan Li et al., "Molecular Mechanisms of PFOA-Induced Toxicity in Animals and Humans: Implications for Health Risks," *Environment International*, vol. 99, pp. 43-54, 2017. [CrossRef] [Google Scholar] [Publisher Link]

[10] Sze Yee Wee, and Ahmad Zaharin Aris, "Revisiting the "Forever Chemicals", PFOA and PFOS Exposure in Drinking Water," *NPJ Clean Water*, vol. 6, no. 1, pp. 1-16, 2023. [CrossRef] [Google Scholar] [Publisher Link]

[11] Minkyu Park et al., "Adsorption of Perfluoroalkyl Substances (PFAS) in Groundwater by Granular Activated Carbons: Roles of Hydrophobicity of PFAS and Carbon Characteristics," *Water Research*, vol. 170, 2020. [CrossRef] [Google Scholar] [Publisher Link]

[12] Jun-Meng Jian et al., "Global Distribution of Perfluorochemicals (PFCS) in Potential Human Exposure Source – A Review," *Environment International*, vol. 108, pp. 51-62, 2017. [CrossRef] [Google Scholar] [Publisher Link]

[13] Yijin Yuan et al., "Rapid Photochemical Decomposition of Perfluorooctanoic Acid Mediated by a Comprehensive Effect of Nitrogen Dioxide Radicals and Fe^{3+}/Fe^{2+} Redox Cycle," *Journal of Hazardous Materials*, vol. 388, 2020. [CrossRef] [Google Scholar] [Publisher Link]

[14] Akshay Chandrashekar Parenky et al., "Decomposition of Carboxylic PFAS by Persulfate Activated by Silver Under Ambient Conditions," *Journal of Environmental Engineering*, vol. 146, no. 10, 2020. [CrossRef] [Google Scholar] [Publisher Link]

[15] Junkui Cui, Panpan Gao, and Yang Deng, "Destruction of Per-and Polyfluoroalkyl Substances (PFAS) with Advanced Reduction Processes (ARPS): A Critical Review," *Environmental Science & Technology*, vol. 54, no. 7, pp. 3752-3766, 2020. [CrossRef] [Google Scholar] [Publisher Link]

[16] Yueh-Feng Li et al., "Cationic Surfactants Influencing the Enhancement of Energy Efficiency for Perfluorooctanoic Acid (PFOA) Removal in the Electrocoagulation-Flotation (ECF) System," *Chemosphere*, vol. 318, 2023. [CrossRef] [Google Scholar] [Publisher Link]

[17] Michel Hubert et al., "Per-and Polyfluoroalkyl Substance (PFAS) Removal from Soil Washing Water by Coagulation and Flocculation," *Water Research*, vol. 249, pp. 1-10, 2024. [CrossRef] [Google Scholar] [Publisher Link]

[18] Jiaqing Xiong et al., "The Rejection of Perfluoroalkyl Substances by Nanofiltration and Reverse Osmosis: Influencing Factors and Combination Processes," *Environmental Science: Water Research & Technology*, vol. 7, no. 11, pp. 1928-1943, 2021. [CrossRef] [Google Scholar] [Publisher Link]

[19] Caihong Liu et al., "Evaluating the Efficiency of Nanofiltration and Reverse Osmosis Membrane Processes for the Removal of Per-and Polyfluoroalkyl Substances from Water: A Critical Review," *Separation and Purification Technology*, vol. 302, 2022. [CrossRef] [Google Scholar] [Publisher Link]

[20] Vera Franke et al., "Efficient Removal of Per-and Polyfluoroalkyl Substances (PFASS) in Drinking Water Treatment: Nanofiltration Combined with Active Carbon or Anion Exchange," *Environmental Science: Water Research & Technology*, vol. 5, no. 11, pp. 1836-1843, 2019. [CrossRef] [Google Scholar] [Publisher Link]

[21] Jianhua Zhang et al., "PFAS Removal from Wastewater by in-Situ Formed Ferric Nanoparticles: Solid Phase Loading and Removal Efficiency," *Journal of Environmental Chemical Engineering*, vol. 9, no. 4, 2021. [CrossRef] [Google Scholar] [Publisher Link]

[22] Shan Huang, and Peter R. Jaffé, "Defluorination of Perfluorooctanoic Acid (PFOA) and Perfluorooctane Sulfonate (PFOS) by Acidimicrobium Sp. Strain A6," *Environmental Science&Technology*, vol. 53, no. 19, pp. 11410-11419, 2019. [CrossRef] [Google Scholar] [Publisher Link]

[23] Melany Ruiz-Urigüen et al., "Biodegradation of PFOA in Microbial Electrolysis Cells by Acidimicrobiaceae Sp. Strain A6," *Chemosphere*, vol. 292, 2022. [CrossRef] [Google Scholar] [Publisher Link]

[24] L.B. Yi et al., "Isolation, Identification, and Degradation Performance of a PFOA-Degrading Strain," *Genetics and Molecular Research*, vol. 15, no. 2, pp. 235-246, 2016. [Google Scholar]

[25] Li Long et al., "Novel Chitosan–Ethylene Glycol Hydrogel for the Removal of Aqueous Perfluorooctanoic Acid," *Journal of Environmental Sciences*, vol. 84, pp. 21-28, 2019. [CrossRef] [Google Scholar] [Publisher Link]

[26] Beatriz Gomez-Ruiz et al., "Photocatalytic Degradation and Mineralization of Perfluorooctanoic Acid (PFOA) Using a Composite TiO_2–rGO Catalyst," *Journal of Hazardous Materials*, vol. 344, pp. 950-957, 2018. [CrossRef] [Google Scholar] [Publisher Link]

[27] Wedja Timóteo Vieira et al., "Removal of Endocrine Disruptors in Waters by Adsorption, Membrane Filtration and Biodegradation. A Review," *Environmental Chemistry Letters*, vol. 18, no. 4, pp. 1113-1143, 2020. [CrossRef] [Google Scholar] [Publisher Link]

[28] Qiaoying Zhang et al., "Removal of Perfluorooctane Sulfonate from Aqueous Solution by Crosslinked Chitosan Beads: Sorption Kinetics and Uptake Mechanism," *Bioresource Technology*, vol. 102, no. 3, pp. 2265-2271, 2011. [CrossRef] [Google Scholar] [Publisher Link]

[29] Yanyan Gong et al., "Removal of Aqueous Perfluorooctanoic Acid (PFOA) Using Starch-Stabilized Magnetite Nanoparticles," *Science of the Total Environment*, vol. 562, pp. 191-200, 2016. [CrossRef] [Google Scholar] [Publisher Link]

[30] Aiza Farhani Zakaria et al., "Recent Advances in Applications of Hybrid Natural Polymers as Adsorbent for Perfluorinated Compounds Removal–Review Paper," *Journal of Polymer Research*, vol. 29, 2022. [CrossRef] [Google Scholar] [Publisher Link]

[31] Xiaole Zhang et al., "Chitosan-Coated Octadecyl-Functionalized Magnetite Nanoparticles: Preparation and Application in Extraction of Trace Pollutants from Environmental Water Samples," *Analytical Chemistry*, vol. 82, no. 6, pp. 2363-2371, 2010. [CrossRef] [Google Scholar] [Publisher Link]

[32] Siphesihle Mangena Khumalo et al., "Application of Response Surface Methodology on Brewery Wastewater Treatment Using Chitosan as a Coagulant," *Water*, vol. 15, no. 6, pp. 1-13, 2023. [CrossRef] [Google Scholar] [Publisher Link]

[33] Agnieszka Sobczak-Kupiec et al., "Review of the Applications of Biomedical Compositions Containing Hydroxyapatite and Collagen Modified by Bioactive Components," *Materials*, vol. 14, no. 9, pp. 1-51, 2021. [CrossRef] [Google Scholar] [Publisher Link]

[34] Shahab Karimifard, and Mohammad Reza Alavi Moghaddam, "Enhancing the Adsorption Performance of Carbon Nanotubes with a Multistep Functionalization Method: Optimization of Reactive Blue 19 Removal through Response Surface Methodology," *Process Safety and Environmental Protection*, vol. 99, pp. 20-29, 2016. [CrossRef] [Google Scholar] [Publisher Link]

[35] Nhlanganiso Ivan Madondo, Sudesh Rathilal, and Babatunde Femi Bakare, "Utilization of Response Surface Methodology in Optimization and Modelling of a Microbial Electrolysis Cell for Wastewater Treatment Using Box–Behnken Design Method," *Catalysts*, vol. 12, no. 9, pp. 1-20, 2022. [CrossRef] [Google Scholar] [Publisher Link]

[36] Marcos Almeida Bezerra et al., "Response Surface Methodology (RSM) as a Tool for Optimization in Analytical Chemistry," *Talanta*, vol. 76, no. 5, pp. 965-977, 2008. [CrossRef] [Google Scholar] [Publisher Link]

[37] S.SD. Elanchezhiyan, and Sankaran Meenakshi, "Encapsulation of Metal Ions Between the Biopolymeric Layer Beads for Tunable Action on Oil Particles Adsorption from Oily Wastewater," *Journal of Molecular Liquids*, vol. 255, pp. 429-438, 2018. [CrossRef] [Google Scholar] [Publisher Link]

[38] Yuanhang Zhan, and Jun Zhu, "Response Surface Methodology and Artificial Neural Network-Genetic Algorithm for Modeling and Optimization of Bioenergy Production from Biochar-Improved Anaerobic Digestion," *Applied Energy*, vol. 355, 2024. [CrossRef] [Google Scholar] [Publisher Link]

[39] Mahmood Alimohammadi et al., "Adsorptive Removal of Arsenic and Mercury from Aqueous Solutions by Eucalyptus Leaves," *Water, Air, & Soil Pollution*, vol. 228, pp. 1-27, 2017. [CrossRef] [Google Scholar] [Publisher Link]

[40] Douglas C. Montgomery, *Design and Analysis of Experiments*, John Wiley & Sons, pp. 1-726, 2017. [Google Scholar] [Publisher Link]

[41] Fei Wang, and Kaimin Shih, "Adsorption of Perfluorooctanesulfonate (PFOS) and Perfluorooctanoate (PFOA) on Alumina: Influence of Solution pH and Cations," *Water Research*, vol. 45, no. 9, pp. 2925-2930, 2011. [CrossRef] [Google Scholar] [Publisher Link]

[42] Luciana Vera Candioti et al., "Experimental Design and Multiple Response Optimization. Using the Desirability Function in Analytical Methods Development," *Talanta*, vol. 124, pp. 123-138, 2014. [CrossRef] [Google Scholar] [Publisher Link]